

Development of sulconazole-loaded nanoemulsions for enhancement of transdermal permeation and antifungal activity

This article was published in the following Dove Press journal:
International Journal of Nanomedicine

Qing Yang^{1,2,*}
Shanshan Liu^{3,*}
Yongwei Gu^{1,2}
Xiaomeng Tang³
Ting Wang^{1,2}
Jianhua Wu⁴
Jiyong Liu¹⁻³

¹Department of Pharmacy, Fudan University Shanghai Cancer Center, Shanghai 200032, People's Republic of China; ²Department of Oncology, Shanghai Medical College, Fudan University, Shanghai 200032, People's Republic of China; ³Department of Pharmacy, Changhai Hospital, Second Military Medical University, Shanghai 200433, People's Republic of China; ⁴Department of Dermatology, Changhai Hospital, Second Military Medical University, Shanghai 200433, People's Republic of China

*These authors contributed equally to this work

Correspondence: Jianhua Wu
Department of Dermatology, Changhai Hospital, Second Military Medical University, Shanghai 200433, People's Republic of China
Tel/Fax +86 213 116 1562
Email wujh_ch@163.com

Jiyong Liu
Department of Pharmacy, Fudan University Shanghai Cancer Center, Shanghai, 200032, People's Republic of China
Tel/Fax +86 213 116 2316
Email liujiyong999@126.com

Background: Sulconazole (SCZ) is a broad-spectrum transdermally administered anti-fungicidal agent. However, the therapeutic effect of SCZ is generally limited by its poor water solubility. This present study aimed to develop and evaluate sulconazole-loaded nanoemulsions (SCZ-NEs) for enhancement of the transdermal permeation and antifungal activity.

Methods: A spontaneous titration method was applied to prepare the SCZ-NEs. And the optimized formulation of SCZ-NEs was screened by central composite design (CCD). In addition, the characteristics of the SCZ-NEs were evaluated, including particle size, zeta potential, drug loading (DL%) and encapsulation efficiency (EE%). The morphology of SCZ-NEs was observed by transmission electron microscopy (TEM). Franz diffusion cells were used to evaluate the transdermal permeability of the SCZ-NEs. The antifungal activity of the SCZ-NEs was measured by a zone of inhibition (ZOI) test.

Results: The optimized SCZ-NEs possessed a moderate particle size of 52.3±3.8 nm, zeta potential of 23.3±1.2 mV, DL% of 0.47±0.05% and EE% of 87.1±3.2%. The ex vivo skin permeation study verified that the cumulative permeability (Q_n) and penetration rate (J_s) of the optimized SCZ-NEs were about 1.7-fold higher than that of a commercial reference, miconazole (MCZ) cream and 3-fold higher than that of SCZ-DMSO solution. The optimized SCZ-NEs exhibited zone of inhibition (ZOI) values of 23.5±2.4 and 20.4±2.5 mm against *C. albicans* and *T. rubrum*, which were larger compared with these of the MCZ cream and SCZ-DMSO solution.

Conclusion: SCZ-NEs were effectively developed to overcome the poor solubility of SCZ, promote SCZ permeation through the skin and improve its antifungal activity. Thus, the SCZ-NEs are a promising percutaneous administration for skin fungal infections induced by *C. albicans* and *T. rubrum*.

Keywords: sulconazole, nanoemulsion, central composite design, transdermal delivery, antifungal activity

Introduction

As broad-spectrum antifungal drugs are widely used, the emergence of resistant fungal strains in clinical cases has become a major problem in antifungal therapy. Therefore, the research and development of novel antifungal drug systems that have not been extensively in clinical settings is highly valued.

Sulconazole (SCZ) is a broad-spectrum anti-fungicidal transdermally administered agent for treating skin infections, including dermatophyte infections, pityriasis versicolor and candidiasis with rare clinical use.¹ In some trials, SCZ produced

better antifungal activity than other drugs (Miconazole and Clotrimazole) for the treatment of candidiasis and tinea pedis.² SCZ has shown promising prospects in preliminary clinical practice and might be a succedaneum or used in combination with other drugs, especially in cases where existing antifungal drugs have not been effective.³ However, the therapeutic efficacy of SCZ has been limited by its poor water solubility. The development of specifically designed drug delivery systems for SCZ has been considered the primary method for addressing the issues.

Nanocarriers including liposomes, transferosomes, vesicles, lipid nanoparticles, polymer micelles and nanoemulsions are widely used in transdermal drug delivery system (TDDS). These nanocarriers, which promote drug penetration and stability, have been widely used to overcome the drawback of poorly water-soluble drugs.⁴ Nanoemulsions (NEs), which have simple preparation, can improve drug penetration and have high solubilization for lipophilic and hydrophilic drugs, was selected as the drug carrier in this study.⁴ The transdermal mechanism of NEs mainly includes disordering the lipid bilayer of the stratum corneum, increasing the solubility of the drug, and strengthening the hydration of the stratum corneum.^{5,6} Previous studies have shown that NEs with small particle size, positive surface charge and sufficient drug loading could effectively penetrate into skin.^{5,7}

The composition of NEs plays a major role in promoting drug percutaneous permeability. The oil phase occupies a critical position in oil-in-water (O/W) NEs formation because it solubilizes the lipid-soluble drugs to generate a therapeutic effect. Surfactants can improve the permeability of a drug delivery system by destroying the lipid bimolecular structure of the stratum corneum. Cosurfactants can assist surfactants by reducing the interfacial tension for the spontaneous formation of NEs.^{8,9} The presence of water enhances the liquidity of the formulation and facilitates drug penetration.

In addition, NEs have been widely studied as antifungal drug delivery carriers and have shown promising abilities for enhancing drug loading, improving antifungal efficacy and targeting infected tissues.¹⁰ From a previous in vitro assay, the antifungal activity of drug loaded in NEs was significantly improved compared with the activity of the drug in solution. The large specific surface area contributed to the drug's interaction with ergosterol.^{11,12} Thus, NEs are considered a promising antifungal drug delivery carrier.

There have been no reports on the specific design of a drug delivery system for SCZ, and no commercial SCZ formulation for clinical. In this study, we prepared NEs for loading SCZ to overcome the poor solubility of SCZ, promote SCZ permeation through the skin and improve its antifungal efficiency, and we assessed the improvements in transdermal permeability and antifungal activity of the SCZ-NEs compared with miconazole cream, which is a commonly used antifungal agent.

Materials and methods

Materials

Sulconazole (SCZ) was obtained from Second Military Medical University. Propylene glycol was purchased from Shanghai Yuanye Biological Technology Co., Ltd (Shanghai, China). Capryol 90, labrafil and labrasol were purchased from Gattefosse (Saint-Priest, France). Soybean oil, olive oil, castor oil, tween 80, EL-40 and polyethylene glycol 400 were purchased from Huanye Pharmaceutical Co., Ltd. (Guangzhou, China). Isopropyl myristate and medium chain triglycerides (MCT) were obtained from Lipoid GmbH (Ludwigshafen, Germany). Ethyl oleate was purchased from Sinopharm Chemical Reagent Co., Ltd. (Beijing, China). Commercial miconazole (MCZ) cream (Daktarin®, sold in Chinese market) was purchased from Xian Janssen Pharmaceutical Co., Ltd (Xian, China). All other materials and solvents were of analytical grade. Fungal strains of *Candida albicans* and *Trichophyton rubrum* were purchased from Tongji University (Shanghai, China).

Animals

All animal protocols complied with the Guide for the Care and Use of Laboratory Animals and Institute of Laboratory Animal Resources and were approved by the Institutional Animal Care and Use Committee of Second Military Medical University. Male SD rats weighing 200–250 g were purchased from the Second Military Medical University. The animal experiments coincided with protocols evaluated by the ethics committee of the Second Military Medical University.

Quantification of SCZ

A UV spectrophotometer was applied to determine the maximum absorption wavelength of SCZ with acetonitrile as the blank control. The quantity of SCZ was analyzed by HPLC (Agilent 1200, USA). The optimum chromatographic

conditions were as follows. An Agilent ODS C18 column (250×4.6 mm, 5 μm) was used; the mobile phase was a composition of acetonitrile and water –0.5% triethylamine (85:15, v/v); the UV detection wavelength and flow rate were 230 nm and 1 mL/min; the column temperature was set to 25°C. The HPLC method was validated according to the ICH guidelines.

Preparation of SCZ-NEs

Screening of NE ingredients

To achieve acceptable drug loading of SCE-NEs, the oils, surfactants and co-surfactants were selected on the basis of their ability to provide good solubilization for SCZ.⁸ Excess amounts of SCZ were added to different oils, surfactants and co-surfactants. Then, the samples were ultrasonically treated at room temperature for 1 hr and centrifuged at 8000 rpm for 20 mins, and then the supernatant was filtered through a membrane filter (0.45 μm). The SCZ saturation solubilities in oil, surfactant, co-surfactant were measured by HPLC.

Pseudo-ternary phase diagram

The surfactants and co-surfactants were critical constituents for the development of NEs and were used to modify the oil-water interfacial tension of the NE system.¹³ A pseudo-ternary phase diagram was applied to screen the ratio of surfactant to co-surfactant (K_m) for SCZ-NE system.¹⁴ Briefly, mixtures of surfactants and co-surfactants (S_{mix}) with different weight ratios ($K_m=2:1, 1:1, 1:2$, respectively) were mixed with the selected oil phase at different weight ratios of 1:9, 2:8, 3:7, 4:6, 5:5, 6:4, 7:3, 8:2 and 9:1. Each combination was titrated slowly with distilled water under magnetic stirring at 300 rpm until the solution became clear. A pseudo-ternary phase diagram was constructed according to the ratios of oil, S_{mix} and distilled water.

Screening the ratio of oil and mixed-surfactant

Formulations of SCZ-NE (NE1-NE5) were prepared with different oil: S_{mix} ratios (1:9, 2:8, 3:7, 4:6, 5:5, respectively) and the physicochemical properties, such as particle size, polydispersity index (PDI) and appearance stability, were measured to pre-screen the ratio of oil and mixed-surfactant.

Screening the proportion of aqueous phase

Formulations of SCZ-NE (NE6-NE8) were prepared with the pre-screened ratio of oil and mixed-surfactant and 30%, 50%, 70% proportions of aqueous phase, respectively. The physicochemical properties, such as particle size, PDI and

appearance stability, were evaluated to screen the proportion of the aqueous phase in the NE system.

Optimization of SCZ-NEs by central composite design (CCD)

Based on the above single-factor studies, the ratio of oil to mixed-surfactant and the proportion of the aqueous phase had a substantial influence on the properties of the SCZ-NEs. Thus, these two factors were selected as independent variables for the optimization experiment.

Central composite design (CCD) was applied to optimize the formulation of SCZ-NEs with the Design Expert[®] software (Version 7). A two-factor, five-level CCD experiment was developed. The ratio of oil to mixed-surfactant (X_1) and the proportion of the aqueous phase (X_2) were selected as the independent variables. The encapsulation efficiency (EE%, Y_1), drug loading (DL%, Y_2), particle size (Y_3) and zeta potential (Y_4) were selected as the dependent variables.

The total number of experimental runs was calculated from Eq. (1):¹⁵

$$2^k + 2k + n_0 \quad (1)$$

where k is the number of independent variables, 2^k is the number of factorial runs, $2k$ is the number of axial runs and n_0 is the number of repeated replications of the center point.¹⁶ A desirability function is typically used to combine multiple responses (Y_i) into a single response using mathematical methods. The desirability value (D) varies from 0 to 1. A desirability value close to 1 indicates a high degree of satisfaction for the corresponding response. The desirability value was calculated from Eqs. (2) and (3):¹⁷

$$d_i = (Y_i - Y_{\min i}) / (T_i - Y_{\min i}) \quad (Y_{\min i} \leq Y_i \leq T_i)$$

$$d_i = (Y_{\max i} - Y_i) / (Y_{\max i} - T_i) \quad (T_i \leq Y_i \leq Y_{\max i}) \quad (2)$$

$$D = (d_1 \times d_2 \times \dots \times d_i) / i \quad (3)$$

$Y_{\min i}$ and $Y_{\max i}$ represent the lower and upper limits of the response (Y_i), T_i represents the target value of the response (Y_i) (T_i value for Y_1, Y_2 and Y_4 were large, T_i value for Y_3 was small), and d_i represents the desirability value of an individual response (Y_i) for a single run.

Characterization of SCZ-NEs

Particle size, PDI and zeta potential

The particle size, PDI and zeta potential of SCZ-NEs were measured by a Malvern-Zetasizer/Nanosizer (Malvern,

Worcestershire, UK). All formulations were measured at 25°C, and each sample was analyzed in triplicate.

Transmission electron microscopy (TEM)

The morphology and microscopic appearance of SCZ-NEs were observed by transmission electron microscopy (TEM, 100CXII, Japan). A droplet of a SCZ-NE solution was deposited for 3 mins onto a copper grid covered with Formvar membrane. The grid was observed by TEM after drying.

Drug loading (DL%) and encapsulation efficiency (EE%)

The DL% and EE% of SCZ-NEs were studied by centrifugation.¹⁸ To separate the unencapsulated drug from the SCZ-NEs, 1 mL of a SCZ-NE solution was centrifuged at 12,000 rpm at 4°C for 20 mins. The supernatant was filtered through a 0.45 µm filter and measured by HPLC. The DL% and EE% of the SCZ-NEs were calculated using the following Eqs. (4) and (5):

$$DL(\%) = (W_{\text{Total}} - W_{\text{Free}}) / W_{\text{NE}} \times 100\% \quad (4)$$

$$EE(\%) = (W_{\text{Total}} - W_{\text{Free}}) / W_{\text{Total}} \times 100\% \quad (5)$$

The W_{Total} represents the weight of SCZ added to the NEs, W_{Free} represents the weight of SCZ unencapsulated by the NEs, and W_{NE} represents the weight of the NE system.

Stability study

The short-term and physical stability studies were used to evaluate stabilities of the SCZ-NEs. In the short-term stability study, the prepared SCZ-NEs were stored at room temperature for 14 days. The particle size, zeta potential, EE% and DL% of the SCZ-NEs were measured at predetermined time intervals (0th, 7th and 14th day).¹⁹ Additionally, the SCZ-NEs were centrifuged at 10,000 rpm for 30 mins to evaluate their physical stabilities.

Ex vivo skin permeation study

Franz diffusion cell was used to conduct the skin permeation study. The transdermal permeabilities of the SCZ-NEs were evaluated in comparison to MCZ cream with a SCZ-DMSO solution as the control group. The SD rats (200–250 g) were anesthetized, and the abdominal skin of the rats was depilated and surgically dissected. The skin samples were fixed between the donor and acceptor chamber with effective diffusion area of 0.85 cm². The receptor medium was a mixture of phosphate-buffered saline (PBS, pH=7.4) and methanol (70:30, v/v) to meet sink conditions. The acceptor

chamber was kept at 32°C and stirred at 400 rpm. Equivalent weights (1 mg) of each formulation were applied onto the skin for 12 hrs. Then, 1 mL of the receptor medium was extracted at 1, 2, 4, 6, 8, 10 and 12 hrs. Additionally, an equal volume of fresh acceptor medium was added to the acceptor chamber. Samples taken at different time points were quantified by HPLC analysis after centrifuging at 12,000 rpm for 10 mins.

The cumulative amount of permeation (Q_n) was plotted on the Y-axis with the transdermal time on the X-axis to construct a transdermal absorption curve. The slope of the linear region of the curve was considered the penetration rate (J_s). The parameters of Q_n , J_s and K_p (permeability coefficient) were calculated from Eqs. (6), (7) and (8):²⁰

$$Q_n = (C_n \times V_0 + \sum_{i=1}^{n-1} C_i \times V_i) / S \quad (6)$$

$$J_s = dQ_n / dt \quad (7)$$

$$K_p = J_s / C_0 \quad (8)$$

where C_n represents the SCZ concentration of the extracted receptor medium, C_i represents SCZ concentration of the sample, V_0 and V_i represent the volume of the receptor medium and sample, respectively, S represents the effective penetration area, C_0 represents the SCZ concentration in the formulation.

Antifungal activity

C. albicans and *T. rubrum* were selected as experimental strains. The zones of inhibition (ZOI) were measured to assess the antifungal efficiencies of the SCZ-NEs. The ZOI test was divided into four groups. Groups A, B, C and D were the SCZ-NEs, MCZ cream, SCZ-DMSO solution and Blank NEs, respectively (Group A: test group, SCZ-NEs (0.5% w/v); Group B: positive control group, MCZ cream (0.5% w/v); Group C: control group, SCZ-DMSO solution (0.5% w/v); Group D: blank control group, blank NEs). The MCZ cream, which is commonly used in clinical practice, was used as a positive control. Inoculum suspensions of *C. albicans* and *T. rubrum* were diluted with RPMI-1640 to a concentration of 1–5 × 10⁶ colony forming units per mL (CFU/mL), as counted with a Neubauer Chamber. Then, 100 µL of inoculum suspensions were evenly inoculated onto a Sabouraud agar plate (9 cm in diameter). The samples were loaded into a well (diameter of 6 mm). Then, the plates were incubated at 35 ± 2°C for 48 hrs. The antifungal efficiency was

assessed from the range of inhibition of fungal growth around the drug solution. The ZOL values were measured in millimeters.

Data analysis

One way analysis of variance (ANOVA) or paired-sample *t*-test was used to analyze the statistical data by SPSS software version 17.0. A *p*-value of 0.05 or less ($p < 0.05$) was considered statistically significant. All data were expressed as the mean value \pm SD ($n=3$).

Results and discussion

Preparation of SCZ-NEs

Solubility study

The DL% and transdermal permeation of SCZ have generally been limited by its poor water solubility. Thus, the selection of suitable components to obtain maximum solubilization of SCZ was a critical step for the preparation of SCZ-NEs, especially for the development of a transdermal drug delivery system (TDDS). The results of the drug solubility tests in various oils, surfactants and co-surfactants are shown in Figure 1, which indicated that SCZ had the maximum drug solubilities in Capryol 90 (0.70 \pm 0.05 mg/g), labrasol (2.88 \pm 0.34 mg/g) and 1,2-propanediol (2.02 \pm 0.15 mg/g). Capryol 90, as a solubility and bioavailability enhancer, showed significantly increased solubilization of SCZ compared with that of IPM, ethyl oleate, soybean oil, olive oil and MCT. SCZ had the highest solubility in labrasol compared with that of other surfactants. In addition,

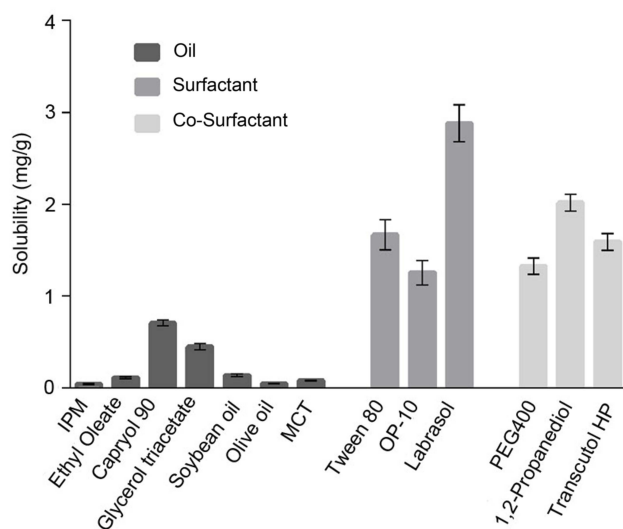


Figure 1 Solubility of SCZ in different oils, surfactants and co-surfactants. Results are represented as the mean \pm SD ($n=3$).

Abbreviations: IPM, isopropyl myristate; MCT, medium chain triglycerides; OP-10, octaphenyl polyoxyethylene-10; PEG400, polyethylene glycol 400.

labrasol has the characteristics of exceptionally low toxicity, excellent solubilization ability and great permeability.²¹ Propylene glycol possessed maximum solubilization for SCZ and was considered the appropriate co-surfactant for preparing the SCZ-NEs. Conclusively, Capryol 90, labrasol and 1,2-propanediol were selected as the best oil, surfactant and co-surfactant compositions, respectively.

Pseudo-ternary phase diagram

Smix with optimal ratio not only enabled the stability of NEs and enlarged the emulsification region of NEs but also reduced the irritation caused by NEs.^{22–24} In this report, the Smix ratios used to form the NEs were screened with a pseudo-ternary phase diagram. The numeric value of emulsifying regions in the pseudo-ternary phase diagram was quantized using Origin[®] (2017). The emulsifying region areas of Km=1:2, Km=1:1 and Km=2:1 were 71.2 \pm 2.1, 80.3 \pm 2.3 and 98.5 \pm 3.1, respectively. According to the calculation results and data in Figure 2, the SCZ-NEs with a Km ratio of 2:1 showed the largest emulsifying region compared to that of the ratios of 1:1 and 1:2, which indicated the SCZ-NEs could more easily spontaneously emulsify and had better stability at a Km ratio of 2:1. Thus, the most appropriate ratio of Km to prepare the SCZ-NEs was 2:1.

Screening the ratio of oil to mixed-surfactant

The physicochemical properties of formulations (NE1-NE5) with different ratios of oil phase to mixed-surfactant are summarized in Table 1. NE1 exhibited good properties, having the smallest particle size (54.2 \pm 3.4 nm), lowest PDI (0.205 \pm 0.02) and good appearance stability compared with those of the other NEs. The results showed that the properties of the SCZ-NEs degraded with decreasing content of surfactant. The results could be explained by comparatively lower contents of surfactant not sufficiently supporting the oil-water interfacial bending energy needed for emulsification.²⁵

Screening the proportion of aqueous phase

The physicochemical properties of formulations (NE6-NE8) with different proportions of the aqueous phase are listed in Table 2. NE8, which had the highest proportion of the aqueous phase, possessed better properties in terms of particle size (36.7 \pm 2.7 nm) and PDI (0.137 \pm 0.02) compared to those of the other NEs.

Based on the above single-factor studies, it could be concluded that the content of oil, surfactants and aqueous phase, to different extents, had a substantial influence on the physical properties of the SCZ-NEs. Thus, there existed the optimal ratios of the components.

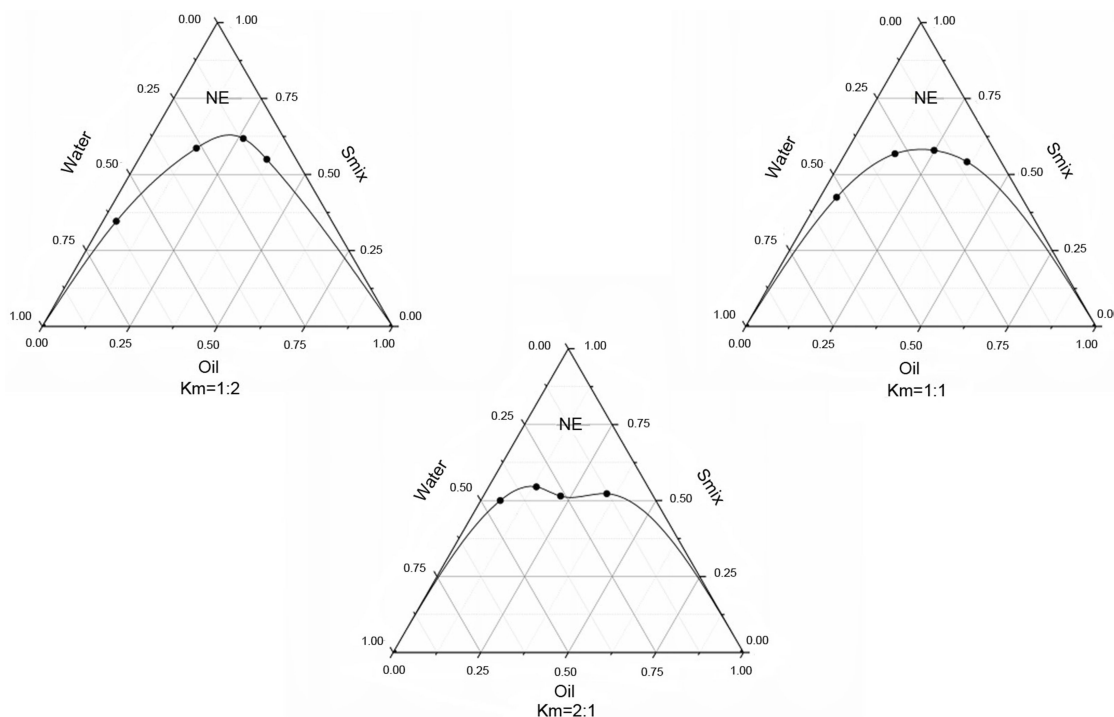


Figure 2 Pseudo-ternary phase diagrams of SCZ-NEs with different Km values (1:2, 1:1 and 2:1).

Abbreviations: SCZ-NEs, sulconazole-loaded nanoemulsions; Smix, mixed-surfactants; Km, surfactant: co-surfactant ratio.

Table 1 Particle size, PDI and appearance stability of SCZ-NEs with different O:S ratios

Formulations	Capryol 90 (%)	Smix (%) (Km=2:1)	Aqueous (%)	Particle size (nm)	PDI	Appearance
NE1	5	45	50	54.2±3.4	0.205±0.02	Limpid
NE2	10	40	50	86.5±5.7	0.256±0.07	Limpid
NE3	15	35	50	154±11.2	0.353±0.06	Limpid
NE4	20	30	50	236±15.6	0.523±0.12	Turbid
NE5	25	25	50	315±19.3	0.696±0.14	Turbid

Note: Results are represented as mean±SD (n=3).

Abbreviations: PDI, polydispersity index; O:S, oil/mixed-surfactant; SCZ-NEs, sulconazole-loaded in nanoemulsions; Smix, mixed-surfactant; km, surfactant:co-surfactant ratio.

Table 2 Particle size, PDI and appearance stability of SCZ-NEs with different proportions of aqueous phase

Formulations	Oil (%)	Smix (%) (Km=2:1)	Aqueous (%)	Particle size (nm)	PDI	Appearance
NE 6	7	63	30	92.1±4.6	0.323±0.05	limpid
NE 7	5	45	50	52.3±3.8	0.213±0.04	limpid
NE 8	3	27	70	36.7±2.7	0.137±0.02	limpid

Note: Results are represented as mean±SD (n=3).

Abbreviations: PDI, polydispersity index; SCZ-NEs, sulconazole-loaded in nanoemulsions; Smix, mixed-surfactant.

Optimization of SCZ-NEs by central composite design

The CCD method was used to screen the final SCZ-NE formulation with the desired properties for further experiment. All independent variables, related coded and real values are listed in Table 3.

The variation range of EE% (Y_1) for the SCZ-NEs in all experimental runs was from 60.20% to 96.20%, as presented in Table 4. The wide range of variation indicated that the EE% (Y_1) was strongly affected by the independent variables. The non-linear model for Y_1 was implied to be significant with an F-value of 8.51, a p -value <0.05 and

Table 3 Range of variables and their levels used in CCD

Independent variables	Unit	Code level				
		-1.41	-1	0	1	1.41
Oil/mixed-surfactants ratio	w/w	1/9	1/8	1/6	1/4	1/3
Proportion of aqueous phase	%	50	55	60	65	70

Note: Optimization experiment was constructed by 2 factors and 5 levels.

Abbreviation: CCD, central composite design.

Table 4 Scheme of the central composite design: independent values, experimental values of the response variables and overall desirability (D)

Runs	Coded values		Responses				Desirability (D)
	X ₁	X ₂	Y ₁	Y ₂	Y ₃	Y ₄	
1	-1	1	82.18	0.41	62.1	23.2	0.69
2	1	-1	88.53	0.36	82.6	15.3	0.38
3	0	0	93.87	0.39	68	19.3	0.63
4	0	-1.41	94.54	0.45	74	18.6	0.69
5	0	0	94.23	0.42	65.6	16.6	0.66
6	-1.41	0	86.57	0.43	45.3	27.3	0.92
7	1.41	0	79.11	0.33	90.7	12.6	0.16
8	-1	-1	84.8	0.41	59.4	25.9	0.77
9	0	0	92.15	0.4	67.3	15.9	0.58
10	1	1	74.3	0.32	73.7	17.2	0.27
11	0	1.41	60.2	0.32	61.3	20.5	0.30
12	0	0	96.2	0.4	69.6	16.4	0.61

Note: Experimental batch included 4 factorial runs, 4 axial runs and 4 center points.

Abbreviations: X₁, oil/mixed-surfactants ratio; X₂, proportion of aqueous phase; Y₁, encapsulation efficiency (%); Y₂, drug loading (%); Y₃, particle size (nm); Y₄, zeta potential (mV).

an R² value of 0.8764. As shown in Table 5, EE% (Y₁) was significantly affected by the proportion of the aqueous phase (X₂, *p*<0.01), while the ratio of oil to mixed-surfactants (X₁, *p*=0.34) did not significantly affect EE% (Y₁).

The measured values for DL% (Y₂) in all experimental runs varied from 0.32% to 0.45%, as listed in Table 4. The non-linear model for Y₂ was implied to be significant with an F-value of 7.97, a *p*-value <0.05 and an R² value of 0.8692. As shown in Table 5, both X₁ (*p*<0.01) and X₂ (*p*<0.05) had a significant effect on Y₂. The negative coefficients of X₁ and X₂ indicated that the DL% would decrease by decreasing the mixed-surfactant content or increasing the aqueous content. This could be explained by the fact that the solubilization for SCZ would decrease at higher aqueous contents and lower mixed-surfactant contents due to its poor water solubility.

The values for particle size (Y₃) varied from 45.3 to 90.7 nm. The wider range of variation indicated that the particle size was highly affected by the independent variables. The non-linear model for Y₃ was implied to be significant with an F-value of 11.53, a *p*-value <0.01 and an R² value of 0.9057. As shown in Table 5, X₁ (*p*<0.01) had a significant effect on Y₃, while X₂ (*p*=0.13) did not significantly affect Y₃. The oil content increased comparatively with decreasing surfactant content, which resulted in a gradually increasing particle size. The results were in agreement with those of a previous study.²⁶

The values for the zeta potential (Y₄) varied from 12.6 to 27.3 mV. The non-linear model for Y₄ was implied to be

Table 5 ANOVA of quadratic model for the EE%, DL%, particle size and zeta potential responses

Factors	Y ₁		Y ₂		Y ₃		Y ₄	
	Coefficient	P-value	Coefficient	P-value	Coefficient	P-value	Coefficient	P-value
Model	-	<0.05*	-	<0.05*	-	<0.01**	-	<0.01**
X ₁	-1.84	0.34	-0.04	<0.01**	12.38	<0.01**	-4.67	<0.0001***
X ₂	-8.18	<0.01**	-0.03	<0.05*	-3.02	0.13	0.24	0.65
X ₁ X ₂	-2.9	0.29	<0.01	0.38	-2.9	0.27	1.15	0.15
X ₁ ²	-5.05	<0.05*	-0.01	0.18	0.59	0.76	1.61	<0.05*
X ₂ ²	-7.78	<0.01**	-0.01	0.18	0.42	0.83	1.41	<0.05*
R ²	0.8764		0.8692		0.9057		0.9466	

Notes: The significance of the effect of independent variables on responses: **P*<0.05; ***P*<0.01; ****P*<0.0001.

Abbreviations: X₁, oil/mixed-surfactants ratio; X₂, proportion of aqueous phase; Y₁, encapsulation efficiency (%); Y₂, drug loading (%); Y₃, particle size (nm); Y₄, zeta potential (mV).

significant with an F-value of 21.27, a p -value <0.01 and an R^2 value of 0.9466. The zeta potential (Y_4) was significantly affected by X_1 ($p<0.0001$), while X_2 ($p=0.65$) did not significantly affect the zeta potential (Y_4).

Three-dimensional (3D) response surface plots were used to simulate the effects of the independent variables on the response values (Figure 3). NEs with smaller particle sizes and higher absolute zeta potentials generated better transdermal permeation.^{7,27} Zeta potential was also considered an indicator of the stability of the dispersed system. NEs with a higher absolute zeta potential value exhibited excellent system stability.^{25,28} Moreover, positively charged droplets would be more beneficial to transdermal permeation than negatively charged droplets.⁷ High values for DL% and EE% reflected the enhanced transdermal permeation.⁵ A formulation with a high DL%, when applied to the skin, could produce a highly permeable concentration gradient, which favored the transfer of SCZ from the nanovehicle to the skin.^{29,30} As summarized earlier, the desired values of DL%, EE% and absolute zeta potential

were large, while that of the particle size was small. After statistical analysis, an optimum batch with 0.99 desirability was recommended by the software, and the optimum levels of X_1 and X_2 were -1.0 and -0.74 , respectively. Consequently, the proportions of Capryol 90, labrasol, 1,2-propanediol and the aqueous phase for the optimized SCZ-NE were 5.4%, 28.9%, 14.4% and 51.3%, respectively.

Characterization of the optimized SCZ-NEs

The particle size, PDI, zeta potential, DL% and EE% characteristics of the optimized SCZ-NE were measured. The particle size of the SCZ-NE remained essentially constant after the incorporation of SCZ, which might account for its poor water solubility, and the drug was internalized by the lipids instead of adhering to the oil-water interface.^{14,32} As shown in measurement results and Figure 4A, the optimized SCZ-NE possessed a particle

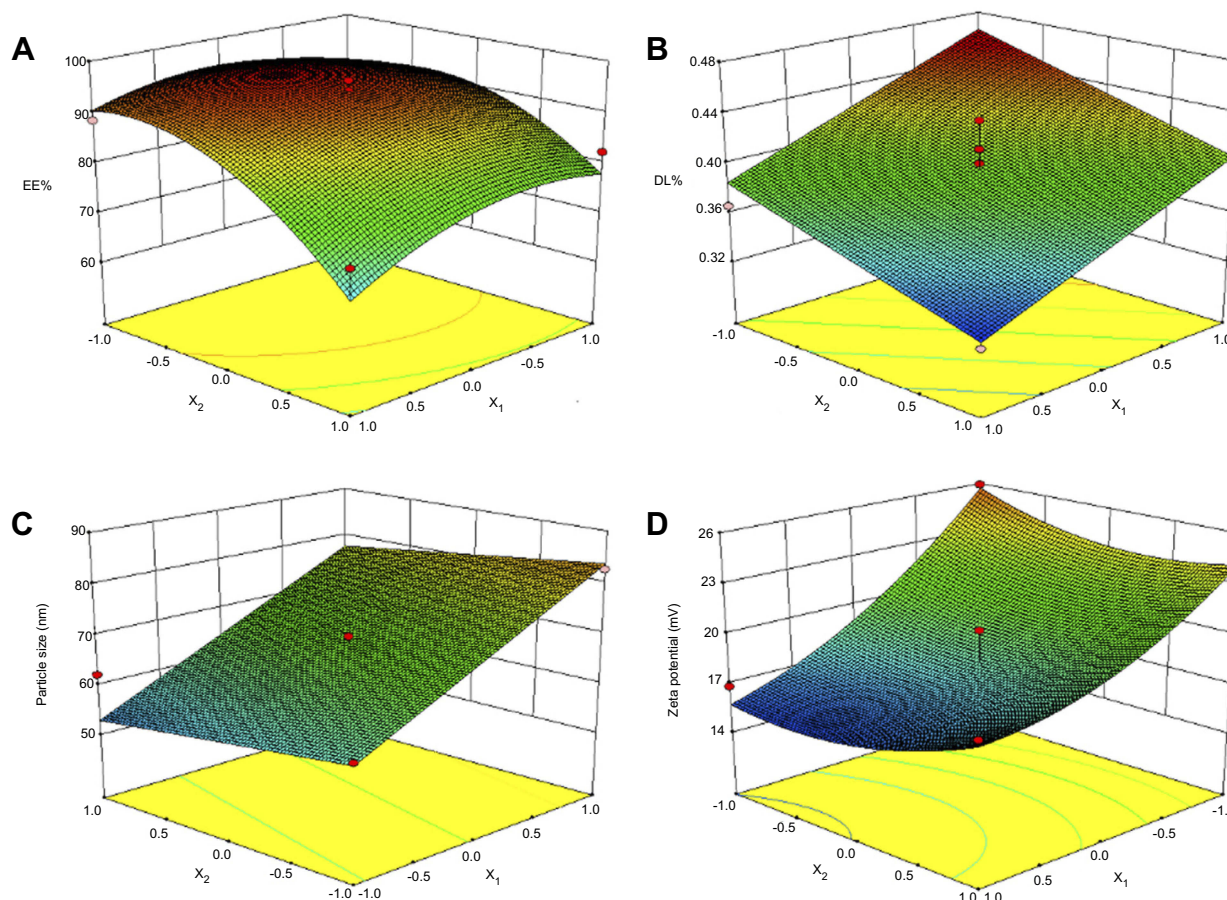


Figure 3 3D surface map of the responses from the central composite design calculations. **(A)** The effects of X_1 and X_2 on EE%. **(B)** The effects of X_1 and X_2 on DL%. **(C)** The effects of X_1 and X_2 on particle size. **(D)** The effects of X_1 and X_2 on zeta potential.

Abbreviations: X_1 , oil/mixed-surfactant ratio; X_2 , proportion of the aqueous phase; EE, encapsulation efficiency (%); DL, drug loading (%)

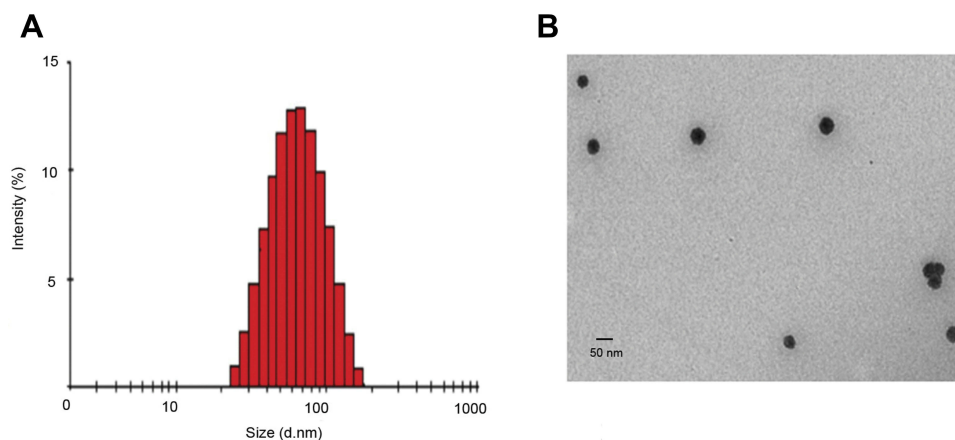


Figure 4 Particle size and morphology of the optimized SCZ-NE. **(A)** Particle size of the optimized SCZ-NE measured by DLS. **(B)** Morphology of the optimized SCZ-NE observed by TEM.

Abbreviations: SCZ-NEs, sulconazole-loaded nanoemulsions; DLS, dynamic light scattering; TEM, transmission electron microscopy.

size of 52.3 ± 3.8 nm, PDI of 0.205 ± 0.02 , zeta potential of 23.3 ± 1.2 mV, DL% of $0.47 \pm 0.05\%$ and EE% of $87.1 \pm 3.2\%$. The DL% of the optimized SCZ-NE was higher compared with that of all 12 runs of the CCD and was especially higher than that of run #6 (highest desirability for all 12 runs). As previously reported, a formulation with a high DL% would favor the transfer of SCZ from the nanovehicle to the skin.^{30,31} TEM is a progressive imaging technique that can precisely observe the morphologies and microscopic sizes of nanosized globules. The spherical morphology of the optimized SCZ-NE is clearly shown in the TEM images in Figure 4B. The particle surface was covered by a thin shell of the surfactants. The TEM images indicated the actual microscopic particle size of the optimized SCZ-NE, and the results were consistent with those obtained from DLS measurements.

Stability study

The particle size, zeta potential, EE% and DL% of the SCZ-NE were measured after 0, 7 and 14 days are listed in Table 6. No significant changes were found in the physicochemical properties of the SCZ-NE during storage, and

Table 6 The particle size, zeta potential, DL% and EE% of the SCZ-NE during 14 days of storage at room temperature

Stability parameters	0th day	7th day	14th day
Particle size (nm)	50.23 ± 3.3	53.51 ± 3.2	51.16 ± 3.6
Zeta potential (mV)	24.62 ± 1.4	23.67 ± 1.6	24.12 ± 1.5
DL%	0.49 ± 0.06	0.48 ± 0.05	0.50 ± 0.03
EE%	88.5 ± 2.3	90.5 ± 2.1	90.9 ± 2.4

Note: Results are represented as mean \pm SD (n=3).

Abbreviations: DL, drug loading; EE, encapsulation efficiency.

the SCZ-NE was still visually transparent. In addition, there was no turbidity or drug precipitation after centrifugation. Therefore, the prepared SCZ-NE exhibited excellent storage stability at room temperature.

Ex vivo skin permeation study

The penetration profiles are shown in Figure 5, and the permeation parameters are listed in Table 7. The results of the penetration profiles of the optimized SCZ-NE showed better transdermal permeation compared with that of the MCZ cream and SCZ-DMSO solution. The permeability rates (J_s) of the SCZ-NE, MCZ cream and SCZ-DMSO solution were 13.7 ± 1.9 , 7.7 ± 1.1 and 4.6 ± 0.4 $\mu\text{g}/\text{cm}^2/\text{hr}$. The permeability rate of the SCZ-NE was 1.76-fold higher than that of the MCZ cream and 2.98-fold higher than that of the SCZ-DMSO solution.

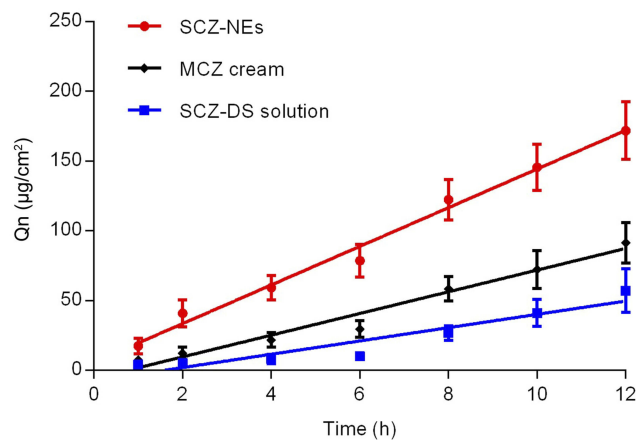


Figure 5 Ex vivo permeation profiles of the SCZ-NE, MCZ cream and SCZ DMSO solution. Results are represented as the mean \pm SD (n=5).

Abbreviations: SCZ-NEs, sulconazole-loaded nanoemulsions; MCZ cream, micronazole commercial reference.

Table 7 The Js, Qn and Kp of SCZ-NE, MCZ cream and SCZ-DMSO solution after permeating for 12 hrs

Parameters	SCZ-DMSO solution	MCZ cream	SCZ-NEs
Qn ($\mu\text{g}/\text{cm}^2$)	57.0 \pm 15.6	91.4 \pm 14.5	171.7 \pm 20.6**:#
Js ($\mu\text{g}/\text{cm}^2/\text{h}$)	4.6 \pm 0.4	7.7 \pm 1.1	13.7 \pm 1.9**:#
Kp $\times 10^{-3}$ (cm/h)	0.9 \pm 0.1	1.5 \pm 0.2	2.7 \pm 0.4**:#

Notes: Results are represented as mean \pm SD (n=3); #P<0.05 vs MCZ cream; **P<0.01 vs SCZ DMSO solution.

Abbreviations: Qn, cumulative penetration quality; Js, penetration rate; Kp, permeability coefficient.

The cumulative amounts of SCZ-NE, MCZ cream and SCZ-DMSO solution that had permeated the skin after 12 hrs were 171.7 \pm 20.6, 91.4 \pm 14.5 and 57.0 \pm 15.6 $\mu\text{g}/\text{cm}^2$, respectively, which indicated that the cumulative permeability of the SCZ-NE was significantly greater than that of the MCZ cream (p<0.05) and SCZ-DMSO solution (p<0.01).

Antifungal activity

The antifungal activity of the SCZ-NE against *C. albicans* and *T. rubrum* was measured by a ZOI test. As shown in Table 8, the ZOIs of the A, B and C groups against *C. albicans* after treatment for 48 hrs were 23.5 \pm 2.4, 17.0 \pm 2.2 and 12.5 \pm 1.9 mm, respectively, and those against *T. rubrum* after treatment for 48 hrs were 20.4 \pm 2.5, 16.8 \pm 2.2 and 13.5 \pm 1.2 mm, respectively. No antifungal activity was found against either *C. albicans* or *T. rubrum* in group D (ZOI=0 mm). Group A, group B and group C all showed

obvious inhibition against *C. albicans* (Figure 6A), and the antifungal efficacy of the SCZ-NE against *C. albicans* was significantly greater than that of the MCZ cream (p<0.05) and SCZ DMSO solution (p<0.01). Additionally, obvious inhibition of *T. rubrum* was also found in group A, group B and group C (Figure 6B). The antifungal efficacy of the SCZ-NE against *T. rubrum* was significantly greater than that of the SCZ DMSO solution (p<0.05) and MCZ cream. Consequently, SCZ-NE exhibited larger ZOIs against *C. albicans* and *T. rubrum* than did the MCZ cream and SCZ DMSO solution, which indicated that the NE, as a nanosized drug carrier loaded with SCZ, showed promising anti-fungal efficacy. From Figure 6, the blank NEs did not show activity against *C. albicans*, and *T. rubrum*, indicating the developed formulation of the SCZ-NE had no innate antifungal efficacy. The SCZ-NE, with its large

Table 8 ZOIs against *C. albicans* and *T. rubrum* for the SCZ-NEs, MCZ cream, SCZ-DMSO solution and Blank NEs after incubation at 30°C for 48 hrs

Groups	Formulations	ZOI (mm)	
		<i>C. albicans</i>	<i>T. rubrum</i>
A	SCZ-NEs	23.5 \pm 2.4* ##	20.4 \pm 2.5#
B	MCZ cream	17.0 \pm 2.2	16.8 \pm 2.2
C	SCZ-DMSO solution	12.5 \pm 1.9	13.5 \pm 1.2
D	Blank NEs	0	0

Notes: Results are represented as mean \pm SD (n=3); *P<0.5 vs Group B; #P<0.5, ##P<0.01 vs Group C.

Abbreviations: ZOI, zone of inhibition; SCZ-NEs, sulconazole-loaded in nanoemulsion; MCZ cream, miconazole commercial reference.

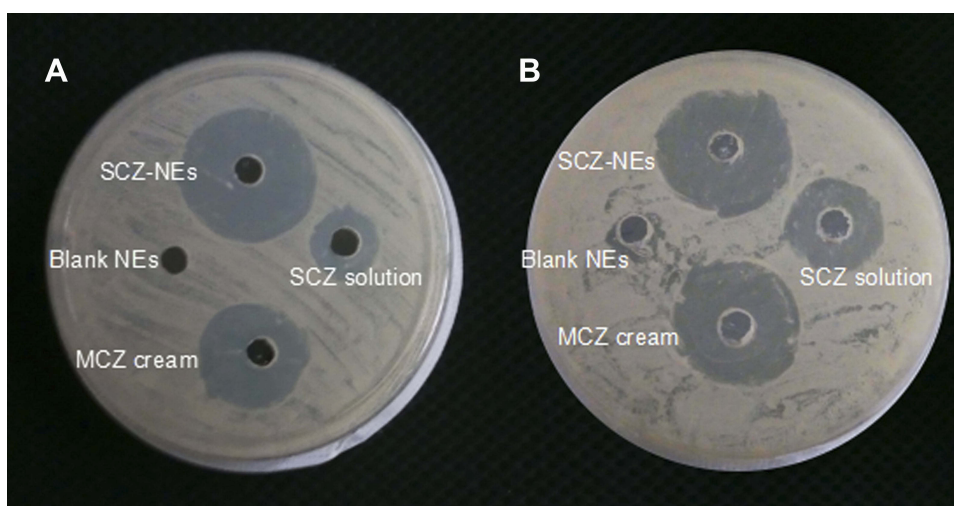


Figure 6 The zones of inhibition for the SCZ-NE, MCZ cream and SCZ DMSO solution. (A) The zones of inhibition for the SCZ-NE, MCZ cream and SCZ DMSO solution against *C. albicans*. (B) The zones of inhibition for the SCZ-NE, MCZ cream and SCZ DMSO solution against *T. rubrum*. The SCZ concentration in each formulation was 5 mg/ml. The results are represented as the mean \pm SD (n=3).

Abbreviations: SCZ-NEs, sulconazole-loaded in nanoemulsion; MCZ cream, miconazole commercial reference.

specific surface area, could easily interact with the surface of the fungal cells and exhibited antifungal effects. The antifungal effects of the SCZ-NE might be related to the ability of the NE to approach the ergosterol composition of fungal hyphae.^{17,31} As previously reported, a novel formulation of Miconazole transdermal films was prepared and exhibited a skin permeability rate of 5.161 $\mu\text{g}/\text{cm}^2/\text{hr}$ and efficient activity ($\text{ZOI}=22.6\pm 2.0$ mm) against *C. albicans*.³³ The SCZ-NE prepared here showed a similar or even better transdermal permeability ($J_s=13.7\pm 1.9$ $\mu\text{g}/\text{cm}^2/\text{hr}$) and antifungal activity ($\text{ZOI}=23.5\pm 2.4$ mm) against *C. albicans*. Additionally, the ingredients of the formulation that were used are easily obtained, and the preparation of the SCZ-NE was simple and convenient.

Conclusions

This study was the first to load SCZ into a NE to improve its transdermal permeation and antifungal efficiency. Central composite design was successfully used to optimize the composition of the SCZ-NE formulation. According to the ex vivo permeation study, the SCZ-NE exhibited significantly higher transdermal permeation than that of the MCZ cream and SCZ-DMSO solution. The nanoscale size and sufficient drug load of the SCZ-NE contributed to the transfer of SCZ from the nanovehicle to the skin. Additionally, the antifungal efficiency of the SCZ-NE against *C. albicans* and *T. rubrum* was greater than that of the MCZ cream and SCZ-DMSO solution. The SCZ-NE showed similar or even better antifungal activity than common clinical drugs. The SCZ-NE prepared in the present study was superior in terms of the ease of availability of the ingredients, simple preparation, excellent stability, and improvement in the skin permeability and antifungal activity compared with those of a commercial antifungal agent. As summarized above, the SCZ-NE is a promising topically administered preparation for the treatment of fungal skin infections.

Acknowledgments

This work was supported by the projects of National Natural Science Foundation of China (81573613, 81873011), the Science and Technology Commission of Shanghai Municipality (16401901900, 18401931500), the Development Fund for Shanghai Talents (201658), the Outstanding Talents Program of Shanghai Health and Family Planning Commission (2018BR27), the Major Military Logistics Research Projects (AWS16023) and

the Open Project Program of State Key Laboratory of Natural Medicines (No. SKLNMKF201809)

Disclosure

The authors report no conflicts of interest in this work.

References

- Gugnani HC, Gugnani A, Malachy O. Sulconazole in the therapy of dermatomycoses in Nigeria. *Mycoses*. 1997;40:139–141.
- Hercelin B, Delaunay-Vantrou M, Alamichel F, Mazza M, Marty JP. Pharmacokinetics of cutaneous Sulconazole nitrate in the hairless rat: absorption, excretion, tissue concentrations. *Eur J Drug Metab Pharmacokinet*. 1993;18:149–154. doi:10.1007/BF03188789
- Zhou YS, Yao JZ, Xing ZF, Li YF. Synthesis and antifungal activity of Sulconazole and its analogues. *Acad J Sec Mil Med Univ*. 1991;12(2):156–159.
- Lawrence MJ, Rees GD. Microemulsion-based media as novel drug delivery systems. *Adv Drug Deliv Rev*. 2000;45:89–121.
- Lane ME, Hadgraft J, Oliveira G, Vieira R, Mohammed D, Hirata K. Rational formulation design. *Int J Cosmet Sci*. 2012;34:496–501. doi:10.1111/j.1468-2494.2012.00747.x
- Lane ME. Skin penetration enhancers. *Int J Pharm*. 2013;447(1–2):12–21. doi:10.1016/j.ijpharm.2013.02.040
- Baspınar Y, Borchert HH. Penetration and release studies of positively and negatively charged nanoemulsions—is there a benefit of the positive charge? *Int J Pharm*. 2012;430:247–252. doi:10.1016/j.ijpharm.2012.03.040
- Rai VK, Mishra N, Yadav KS, Yadav NP. Nanoemulsion as pharmaceutical carrier for dermal and transdermal drug delivery: formulation development, stability issues, basic considerations and applications. *J Control Release*. 2018;270:203–225. doi:10.1016/j.jconrel.2017.11.049
- Zhang J, Bozema M-K. Investigation of microemulsion microstructures and their relationship to transdermal permeation of model drugs: ketoprofen, lidocaine, and caffeine. *Int J Pharm*. 2011;421:34–44. doi:10.1016/j.ijpharm.2011.09.014
- Soliman Ghareb M. Nanoparticles as safe and effective delivery systems of antifungal agents: achievements and challenges. *Int J Pharm*. 2017;523:15–32. doi:10.1016/j.ijpharm.2017.03.019
- Sosa L, Beatriz C, Alvarado Helen L, Nuria B, Oscar D, Calpena Ana C. Amphotericin B releasing topical nanoemulsion for the treatment of candidiasis and aspergillosis. *Nanomedicine*. 2017;13:2303–2312. doi:10.1016/j.nano.2017.06.021
- Hussain A, Singh S, Webster TJ, Ahmad FJ. New perspectives in the topical delivery of optimized amphotericin B loaded nanoemulsions using excipients with innate anti-fungal activities: a mechanistic and histopathological investigation. *Nanomedicine*. 2017;13:1117–1126. doi:10.1016/j.nano.2016.12.002
- Narang AS, Delmarre D, Gao D. Stable drug encapsulation in micelles and microemulsions. *Int J Pharm*. 2007;345:9–25. doi:10.1016/j.ijpharm.2007.08.057
- Silva AE, Barratt G, Chéron M, Egito EST. Development of oil-in-water microemulsions for the oral delivery of amphotericin B. *Int J Pharm*. 2013;454:641–648. doi:10.1016/j.ijpharm.2013.05.044
- Manikan V, Kalil MS, Hamid AA. Response surface optimization of culture medium for enhanced docosahexaenoic acid production by a Malaysian thraustochytrid. *Sci Rep*. 2015;5:8611. doi:10.1038/srep08611
- Lee A, Chaibakhsh N, Rahman MBA, Basri M, Tejo BA. Optimized enzymatic synthesis of levulinate ester in solvent-free system. *Ind Crops Prod*. 2010;32(3):246–251. doi:10.1016/j.indcrop.2010.04.022
- Liu Y, Zhang P, Feng NP, Zhang X, Wu S, Zhao JH. Optimization and in situ intestinal absorption of self-microemulsifying drug delivery system of oridonin. *Int J Pharm*. 2009;365:136–142. doi:10.1016/j.ijpharm.2008.08.009

18. Zhuang CY, Li N, Wang M, et al. Preparation and characterization of vinpocetine loaded nanostructured lipid carriers (NLC) for improved oral bioavailability. *Int J Pharm.* 2010;394(1–2):179–185. doi:10.1016/j.ijpharm.2010.05.005
19. Tsai MJ, Wu PC, Huang YB, et al. Baicalein loaded in tocol nanostructured lipid carriers (tocol NLCs) for enhanced stability and brain targeting. *Int J Pharm.* 2012;423:461–470. doi:10.1016/j.ijpharm.2011.12.009
20. Zhu WW, Yu AH, Wang WH, Dong RQ, Wu J, Zhai GX. Formulation design of microemulsion for dermal delivery of penciclovir. *Int J Pharm.* 2008;360:184–190. doi:10.1016/j.ijpharm.2008.04.008
21. Kreilgaard M, Pedersen EJ, Jaroszewski JW. NMR characterisation and transdermal drug delivery potential of microemulsion systems. *J Control Release.* 2000;69:421–433.
22. Hua L, Weisan P, Jiayu L, Ying Z. Preparation, evaluation, and NMR characterization of vinpocetine microemulsion for transdermal delivery. *Drug Dev Ind Pharm.* 2004;30:657–666. doi:10.1081/DDC-120039183
23. Ali MS, Alam MS, Alam N, Siddiqui MR. Preparation, characterization and stability study of dutasteride loaded nanoemulsion for treatment of benign prostatic hypertrophy. *Iran J Pharm Res.* 2014;13:1125–1140.
24. Li W, Chen H, He Z, Han C, Liu S, Li Y. Influence of surfactant and oil composition on the stability and antibacterial activity of eugenol nanoemulsions. *Food Sci Technol.* 2015;62:39–47.
25. Bali V, Ali M, Ali J. Study of surfactant combinations and development of a pharmacokinetics of cutaneous Sulconazole nitrate in the hairless rat: absorption, excretion, tissue concentrations. *Colloids Surf B.* 2010;76:410–420. doi:10.1016/j.colsurfb.2009.11.021
26. Yuan Jessica S, Alice Y, Nga N, Jacqueline C, Xiao-Yan W, Acosta Edgar J. Effect of surfactant concentration on transdermal lidocaine delivery with linker microemulsions. *Int J Pharm.* 2010;392:274–284. doi:10.1016/j.ijpharm.2010.03.051
27. Callender SP, Mathews JA, Kobornyk K, Wettig SD. Microemulsion utility in pharmaceuticals: implications for multi-drug delivery. *Int J Pharm.* 2017;526:425–442. doi:10.1016/j.ijpharm.2017.05.005
28. Griesser J, Hetényi G, Kadas H, Demarne F, Jannin V, Bernkop-Schnürch A. Self-emulsifying peptide drug delivery systems: how to make them highly mucus permeating. *Int J Pharm.* 2018;538:159–166. doi:10.1016/j.ijpharm.2018.01.018
29. Mitri K, Shegokar R, Gohla S, Anselmi C, Müller RH. Lipid nano-carriers for dermal delivery of lutein: preparation, characterization, stability and performance. *Int J Pharm.* 2011;414:267–275. doi:10.1016/j.ijpharm.2011.05.008
30. Fernández CF, Clares NB, López SO, Alonso MC, Calpena Campmany AC. Evaluation of novel nystatin nanoemulsion for skin candidosis infections. *Mycoses.* 2013;56:70–81. doi:10.1111/j.1439-0507.2012.02202.x
31. Zhang Y, Shang ZH, Gao CH, et al. Nanoemulsion for solubilization, stabilization, and in vitro release of pterostilbene for oral delivery. *AAPS PharmSciTech.* 2014;15:1000–1008. doi:10.1208/s12249-014-0129-4
32. Thakkar Hetal P, Amit K, Dhande Rahul D, Patel Arpita A. Formulation and evaluation of Itraconazole nanoemulsion for enhanced oral bioavailability. *J Microencapsul.* 2015;32:559–569. doi:10.3109/02652048.2015.1065917
33. Ofokansi KC, Kenechukwu FC, Ogbu NN. Design of novel miconazole nitrate transdermal films based on eudragit RS100 and HPMC hybrids: preparation, physical characterization, in vitro and in vivo studies. *Drug Deliv.* 2014;22(8):1078–1085. doi:10.3109/10717544.2013.875604

International Journal of Nanomedicine

Dovepress

Publish your work in this journal

The International Journal of Nanomedicine is an international, peer-reviewed journal focusing on the application of nanotechnology in diagnostics, therapeutics, and drug delivery systems throughout the biomedical field. This journal is indexed on PubMed Central, MedLine, CAS, SciSearch®, Current Contents®/Clinical Medicine,

Journal Citation Reports/Science Edition, EMBASE, Scopus and the Elsevier Bibliographic databases. The manuscript management system is completely online and includes a very quick and fair peer-review system, which is all easy to use. Visit <http://www.dovepress.com/testimonials.php> to read real quotes from published authors.

Submit your manuscript here: <https://www.dovepress.com/international-journal-of-nanomedicine-journal>